Reply

CHUN-CHIEH WU, SHIN-GAN CHEN, JAN-HUEY CHEN, KUN-HSUAN CHOU, AND PO-HSIUNG LIN

Department of Atmospheric Sciences, National Taiwan University, Taipei, Taiwan

(Manuscript received 28 May 2009, in final form 24 June 2009)

1. Introduction

By defining the response functions to represent the steering flow of a tropical cyclone (TC), the adjoint-derived sensitivity steering vector (ADSSV; Wu et al. 2007, hereinafter W07; Wu et al. 2009a, hereinafter W09) identifies the sensitive areas at the observation time that optimally modify the mean steering flow at the verifying (final) time. The technique was originally developed, while combined with other targeted techniques (Wu et al. 2009b), to assist the targeted observations of the Dropwindsonde Observations for Typhoon Surveillance near the Taiwan Region (DOTSTAR) program (Wu et al. 2005) for improving track forecasts of TCs in the western North Pacific Ocean. W09 demonstrated that the ADSSV captures the signals of the influence of the large-scale trough and the subtropical high prior to the recurvature of Typhoon Shanshan (2006), and such a signature is further supported by the potential vorticity (PV) analysis.

Hoover (2009, hereinafter H09) has commented on W09, questioning the appropriateness of the response functions defined in the ADSSV methodology to describe TC steering and the dynamical interpretation of the adjoint-derived sensitivity gradients. Tests were performed in H09 using the Navy Operational Global atmospheric Prediction System (NOGAPS) model and its adjoint to investigate how perturbations in the initial conditions would influence the steering flow of a TC. H09 suggested that perturbations to the final-time location of the TC can have a larger influence on the zonal and meridional steering, and therefore that the response functions used in W09 are likely invalid in the sense that the TC center will shift after the initial conditions have been perturbed.

Corresponding author address: Dr. Chun-Chieh Wu, Dept. of Atmospheric Sciences, National Taiwan University, No. 1, Sec. 4, Roosevelt Rd., Taipei 106, Taiwan.
E-mail: cwu@typhoon.as.ntu.edu.tw

DOI: 10.1175/2009MWR3074.1

In this reply we wish to clarify that the basic concepts associated with the ADSSV in W07 and W09 have been misunderstood and misinterpreted by H09. H09 provided a simple numerical experiment to indicate a well-known fact that the incorrect center would lead to a biased averaged mean flow at the storm center. In this reply, we elaborate that the numerical experiment in H09 makes sense in itself, but does not provide evidence to indicate that the design and interpretation of ADSSV in W07 and W09 are inappropriate.

2. Reply to specific comments

a. The appropriateness of the ADSSV used to describe TC steering

For ADSSV as originally described in W07, the verifying area in which the response functions are defined is an area (e.g., square of 600 km × 600 km) *centered* at the TC location simulated by the nonlinear forward model, the fifth-generation Pennsylvania State University–National Center for Atmospheric Research Mesoscale Model (MM5) at the verifying time. The response functions (R_1 and R_2) are defined to represent the average background flow *steering* a TC at the verifying time within the verifying area. To calculate the ADSSV for a TC, the MM5 nonlinear forward model is first of all used to perform a 48-h simulation. Based on the simulated TC center location at the verifying time, the response functions and the verifying area are defined as stated above. Then, the MM5 adjoint model integrates backward to obtain the gradients of the response functions to the state variables [zonal and meridional winds (u, v), vertical velocity (w), temperature (T), and pressure perturbation (pp)] at the initial time. From the gradients of the response functions to the zonal and meridional wind, the gradient of the response functions to the vorticity (ς) can be further obtained (see the appendix in Kleist and Morgan 2005). That is the sensitivity of the *average background steering flow* at the

verifying time to the vorticity fields at the initial (observing) time. In other words, the ADSSV represents the changes in the mean steering flow at the verifying time with respect to vorticity perturbation at the initial time.

H09 states that the response functions depend partially on the assumption that the TC is at the center of the verifying region as well as on the size of that region. Figure 1 of H09 shows that if the center used to calculate the mean flow is shifted, a biased representative mean flow would be induced, which is a well-known concept. We stress that the ADSSV calculation completely obeys the assumption that the final TC location is at the center of the verifying region. As explained above, the location of the TC (circulation) center at the verifying time is undoubtedly derived from the exact forward model simulation with no ambiguity, because no other procedure needs to be conducted that would lead to small perturbations to the final-time location of the TC.

About the size of the verifying region, the reason to use the square of 600 km $\times$ 600 km to represent the mean flow (the response functions, R_1 and R_2) is to average out the axisymmetric component of the strong cyclonic flow around the TC center as described in W07. This idea basically follows the well-accepted steering concept as in Chan and Gray (1982) and numerous other publications in the literature. In other words, it is well known that TC motion is mainly controlled by large-scale mean environmental flow, which does not vary significantly at the vortex scale near the TC core. Note that the sensitivity test for the size of the verifying region can be shown by Fig. 1. The major patterns of ADSSV with the highest sensitivity would remain the same (see the red vectors in Fig. 1) when the size of the verifying area is changed to a bigger square domain of 1200 km $\times$ 1200 km. We believe that the design of the verifying area in W07 and W09 for calculating the mean steering flow across a TC is representative and physically meaningful. Furthermore, W07 also shows consistency among the sensitive areas associated with reduced (from 36 to 24 and 12 h) lead times (see Fig. 7 of W07), indicating the robustness of the high sensitivity features identified in ADSSV.

b. About the initial perturbed simulation in H09

The experiment performed in H09 shows that the perturbation zonal flow (Fig. 3 of H09) is mainly caused by the shift of the TC center location, but not directly related to the actual change in the TC steering flow. Thus, H09 suggested that the response functions used in W09 must contend with both steering and nonsteering effects related to small perturbations of the development and final-time location of the TC.

First of all, we consider the experiment shown in H09 to be fine in itself. As indicated in Fig. 1 of H09, obviously it can be expected that wind and height fields are different at the verifying region due to the different TC locations in control and perturbed simulations (Fig. 3 of H09). However, the above results did not provide the evidence to indicate that the design and interpretation of ADSSV in W07 and W09 are inappropriate. The key point is that the shift of the TC location at the verifying time is the result of the difference between the first (control) and second (perturbed) simulations in H09. If the forward model is perturbed, the TC would have a new trajectory, likely with a different center location at the verifying time. This finding does not collide with the definition of the response functions and the ADSSV in W07 and W09. As explained in section 2a, for the ADSSV calculation, the TC at the final time is exactly located at the center of the verifying region, while no perturbation is introduced during the ADSSV calculation in both the forward and backward integrations. In other words, the ADSSV shows the sensitivity at the initial time to the TC's steering flow at the verifying time for the unperturbed forward MM5 simulation. It is incorrect in H09 to use his second (perturbed) simulation to infer that the ADSSV may show both steering and nonsteering effects related to small perturbations of the development and final-time location of the TC.

c. About the test for validity of results in H09

In section 4 of H09 (''Test for validity of results''), H09 showed that ΔR_1 (δR_1) is 2.34 (1.94) m s^{-1}, suggesting that the major contribution to the perturbation zonal flow is directly related to a small translation of the TC, not the actual change in the TC steering flow.

Here, we have two issues to address regarding the above validity result. First, we have to reiterate that the above result cannot be linked to the reliability of the ADSSV. The point is that ΔR_1 is related to the second (perturbed) simulation, and the ADSSV only accounts for the sensitivity calculated from the unperturbed MM5 forward simulation as stated in sections 2a,b. Second, obviously, the difference caused by the unrepresentative centers would lead to the result in H09 (such as 82.8% of the total change in the response function, as shown in section 4 of H09). We believe that a more correct calculation would require an estimation of the difference between the two mean flow fields after the axisymmetric flow has been averaged out with respect to the storm centers of the control and perturbed runs, respectively. This is an issue that resulted from the design of the calculation [Eq. (4)] in H09.

Furthermore, in ADSSV, if one would like to investigate the impact on the steering flow from the perturbed

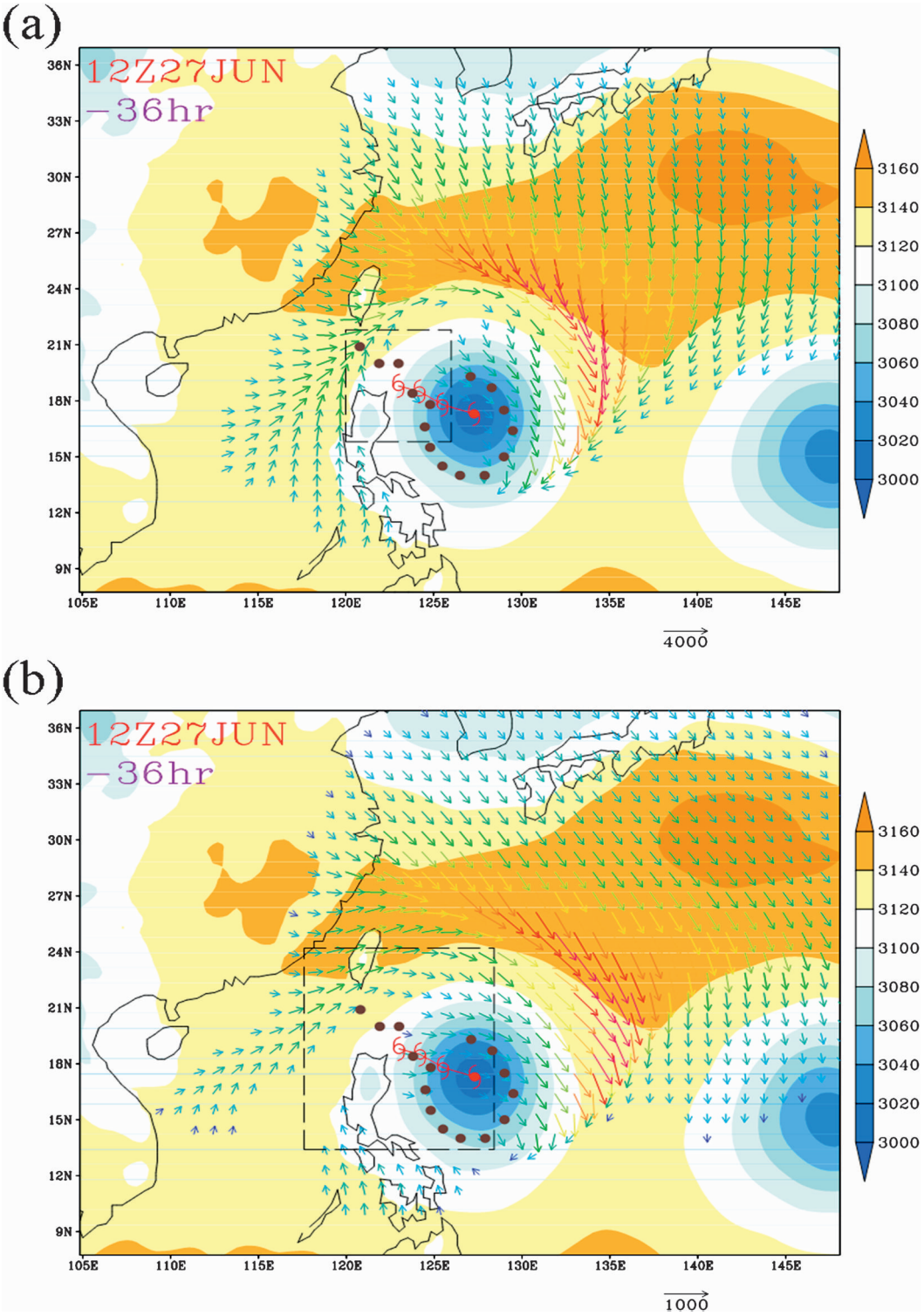

FIG. 1. ADSSV with respect to the vorticity field at 700 hPa at the initial time (1200 UTC 27 June) for Typhoon Mindulle as in the case of W07 calculated from the verifying area of (a) 600 km by 600 km and (b) 1200 km by 1200 km. The background shading is the geopotential height at 700 hPa and the scale of the ADSSV is indicated by the arrow to the lower right (unit: m). The 36-h simulated track is indicated by the typhoon symbols in red for every 12 h. The dots around Mindulle represent the deployed locations of dropwindsondes in DOTSTAR.

model simulation, by design one would calculate the mean steering flow based on the new storm center associated with the perturbed forward model integration. Certainly it would be incorrect to use the unrepresentative storm center from the perturbed run to perform such a calculation. This method should be applied to show the difference between the wind vectors from the unperturbed and perturbed simulations. A more appropriate approach to take in Fig. 3 of H09 is to calculate the difference of the mean steering flow (by removing the axisymmetric wind related to the model storm centers in the unperturbed and perturbed simulations, respectively). In this way, one would be able to see more clearly the impact on the steering flow from the perturbed experiment. This issue is totally independent of the design and calculation of R_1 and R_2 in ADSSV using the well-defined center from the unperturbed forward model run.

d. The dynamical interpretation of the adjoint-derived sensitivity gradients

Note that the PV diagnosis (Wu et al. 2003) applied in W09 provides one approach to investigate the steering contribution from the synoptic weather system indicated by the ADSSV sensitivity. H09 stated that tests need to be performed to determine how perturbations to the initial condition vorticity would impact the steering of Shanshan. Indeed, we have conducted this part of work and are about to submit a follow-up paper reporting our new findings. Here we include some result highlights from our validation experiments in response to the helpful suggestion from H09.

W09 identified the sensitivities associated with the midlatitude trough and the subtropical high from the ADSSV signals (see Fig. 3 of W09), which is well supported by the PV analysis. Here the validation experiments are conducted by comparing the simulations in the forward model between the perturbed and unperturbed initial conditions. The vorticity within the 800-km-radius circle (see Fig. 2 about the initial vorticity perturbation region with center indicated by the symbol X) from the midlatitude trough system is perturbed (e.g., the maximum vorticity associated with the trough at 500 hPa is reduced by 50% from 9.4×10^{-5} s^{-1} to 4.7×10^{-5} s^{-1}; i.e., the perturbation is added to weaken the trough system) following the procedure developed in Wu et al. (2009c) to obtain the dynamically balanced initial flow and mass fields. The perturbed and reduced vorticity between the two circles in Fig. 2 increases in linear proportion with radius and regains its original value at the periphery of a larger circular domain. The forward model is rerun with the newly perturbed initial condition. The perturbed experiment (PERT) is then compared with the unperturbed forecast (CTRL) to validate the impact of the perturbation in the sensitive region (from the ADSSV signal) on the model.

The 850–250-hPa deep-layer-mean (DLM; i.e., steering) winds of CTRL and PERT are calculated by removing the axisymmetric flow relative to the storm centers from CTRL and PERT, respectively. Despite the slight shift of storm centers between CTRL and PERT, the DLM steering flows of CTRL and PERT, respectively, can be easily derived here. The problem of the unrepresentative mean flow due to the use of the incorrect center implied in H09 does not exist in our study. The time evolution of the difference in the DLM steering winds between experiments PERT and CTRL is shown in Fig. 3. The large DLM steering wind difference (with a maximum of about 5 m s^{-1}) at the initial time (Fig. 3a) occurs to the south of the perturbation center and is mainly anticyclonic due to the weakening of the trough in PERT. This anticyclonic flow pattern continues and expands at the 12-h forecast time (Fig. 3b). Following the model integration, the signature of the above DLM wind difference pattern propagates along with the midlatitude trough into the original ADSSV verifying area (as shown in the dashed square box based on the 48-h storm center of CTRL; Figs. 3c–f). In addition, it is also identified that the impact extends to the east of Japan and farther downstream (upper-right features in Figs. 3c–f). It is notable that the initial vorticity perturbation associated with the trough in northern China would 48 h later influence the DLM steering wind around Shanshan in the verifying area.

The comparison between the ADSSV patterns and changes in the DLM steering flow around Shanshan at the verifying time due to the perturbation of the midlatitude trough is conducted here to investigate how perturbations would affect the steering of Shanshan. To compare the difference between the DLM steering flows of CTRL and PERT with the direction of the ADSSV signal near the trough region (see Fig. 2), we calculate the areal average of the DLM steering flows of both CTRL and PERT over the verifying area. (Note that in this case, since the axisymmetric wind component has been removed, the DLM steering wind is generally uniform around the storm. Therefore, the areal average would show no sensitivity to the difference of the storm centers between CTRL and PERT. In other words, the issue raised from the artifact calculation of H09 does not apply here at all.)

In Fig. 4, it is found that the areal-average DLM steering flow in CTRL (thin solid vector) is stronger than that in PERT (thin dashed vector). The difference of DLM steering flows between PERT and CTRL, as indicated by the bold solid vector in Fig. 4, shows a

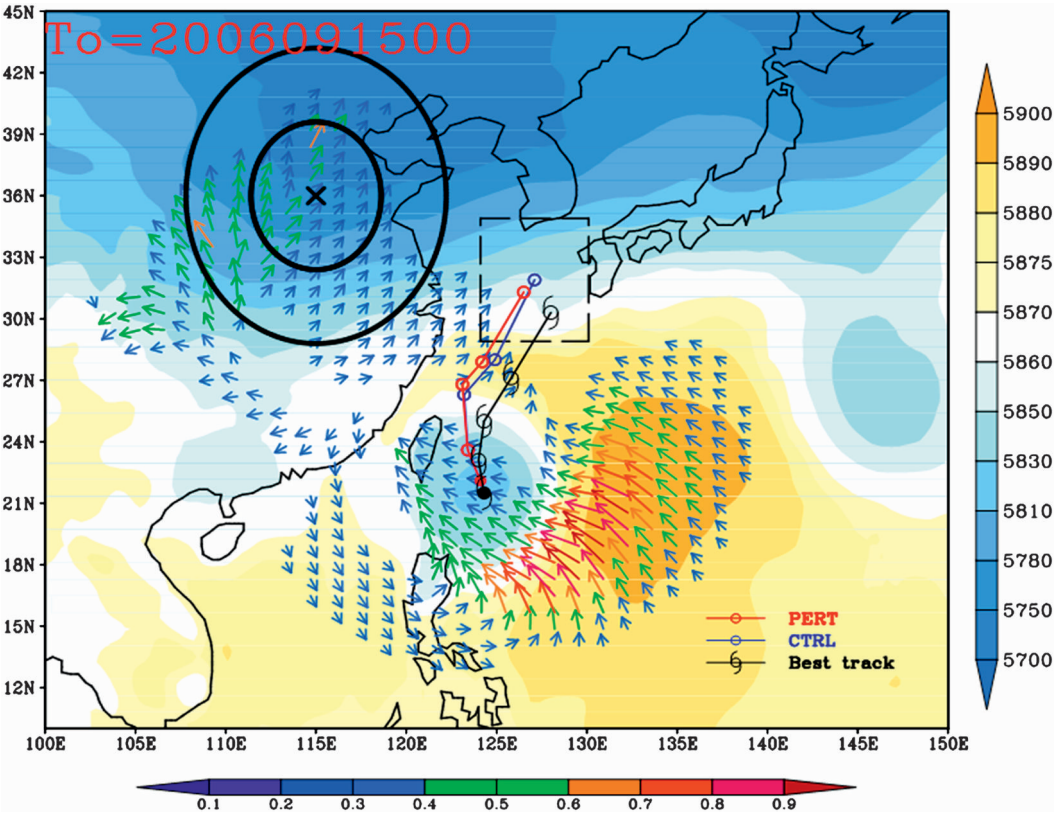

FIG. 2. ADSSV with respect to the vorticity field at 500 hPa at the initial time (0000 UTC 15 September) for Typhoon Shanshan as in Fig. 3b of W09, superposed with the geopotential height at 500 hPa. The X represents the perturbation center in experiment PERT and the two circles are regions with radii of 800 and 400 km. The best track, the simulated tracks of PERT and CTRL are indicated by the black (typhoon symbol), red and blue lines, respectively.

south-southwestward vector, indicating that when the midlatitude trough is weakened at the initial time in PERT, the steering flow at the verifying time is reduced, while the northward movement of Shanshan is also slowed down. This is generally consistent with the signature of the ADSSV averaged over the perturbation region in northern China (see Fig. 2), which is pointing northeastward in Fig. 4 (bold dashed vector), that is, following the definition of ADSSV in W07 and W09, the increase (reduction) of the vorticity at the initial time at the region will lead to change of the mean steering flow toward the northeast (southwest). Again, note that this result has nothing to do with the argument from H09 concerning the problem induced by the different storm center in the perturbed experiment.

3. Final remarks

In this reply, we have clarified the issues raised in H09 concerning the appropriateness of the definition of ADSSV in W07 and W09. We elaborate that the numerical experiment in H09 is fine in itself, but it does not provide evidence to indicate that the design and physical interpretation of ADSSV are inappropriate. Some highlight results from our validation experiments are also included in this reply to address the dynamical interpretation of the ADSSV. The key points are summarized in response to the major issues outlined in the conclusion of H09:

1) Second paragraph of the conclusion of H09, "It has been shown that the response functions used by W09 to describe the zonal and meridional steering of a TC must contend with both steering effects and nonsteering effects related to small perturbations of the development and final-time location of the TC."

   Reply: The key point is that the shift of the TC location at the verifying time is the result of the difference between the first (control) and second (perturbed) simulations in H09. However, for the ADSSV calculation, the TC at the final time is exactly located at the center of the verifying region, while no perturbation is introduced during the

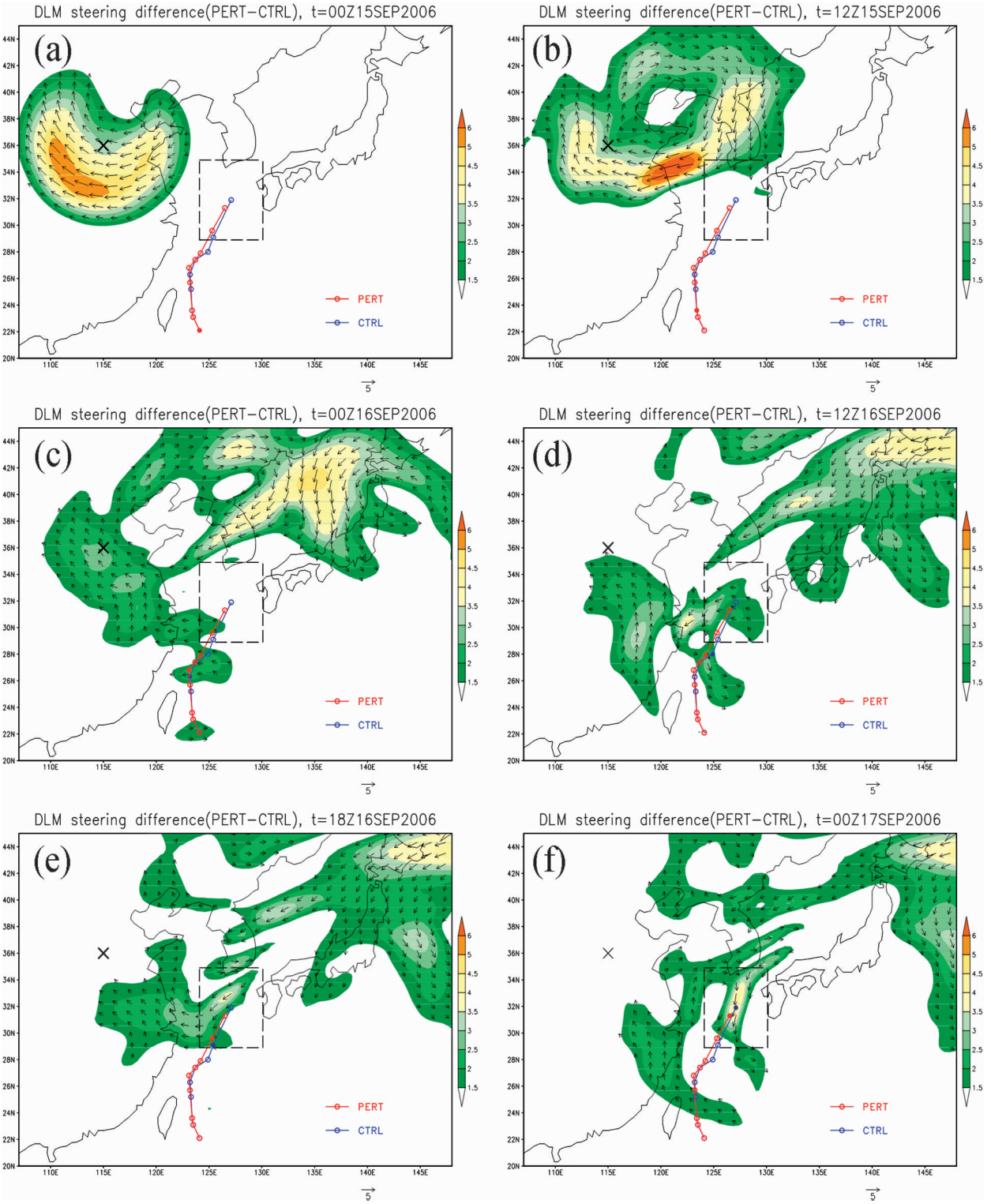

FIG. 3. The difference of the 850–250-hPa DLM steering flow between experiments PERT and CTRL at the forecast time (a) 0, (b) 12, (c) 24, (d) 36, (e) 42, and (f) 48 h initialized at 0000 UTC 15 Sep 2006. Wind with velocity above 1.5 m s^{-1} is shaded and the X over north-central China indicates the perturbation center associated with the midlatitude trough. The simulated tracks for experiments PERT and CTRL are shown in red and blue lines for every 6 h, respectively.

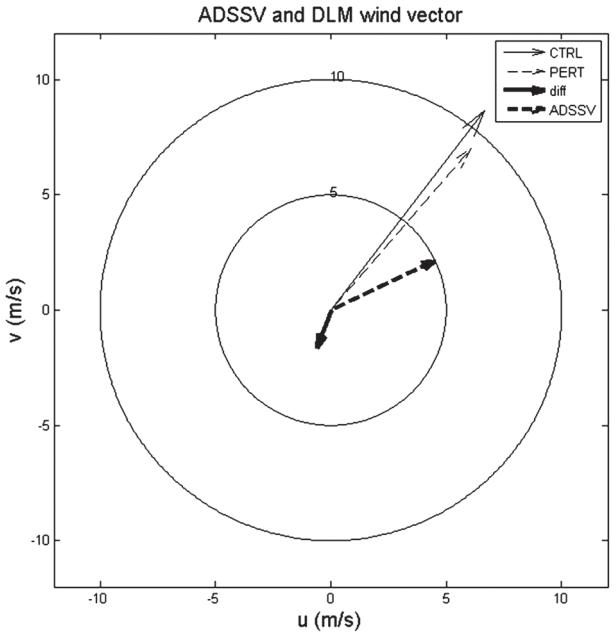

FIG. 4. The areal-average DLM wind vectors within the verifying area at the final time for experiments CTRL (thin solid vector) and PERT (thin dashed vector) after the axisymmetric flow of Shanshan with respect to the storm centers of CTRL and PERT, respectively, is removed. The areal-average DLM wind difference between experiments CTRL and PERT is indicated by the thick solid vector. The ADSSV averaged within the perturbation region is shown by the bold dashed vector and scaled as 5 m. The two circles represent the scales of 5 and 10 m s^{-1}, respectively.

ADSSV calculation in both the forward and backward integrations.

2) Second paragraph of the conclusion of H09, "The influence of nonsteering effects on the sensitivity gradients is dependent on the size of the response function box, as well as perturbations to the intensity, asymmetry, and final-time locations of the TC due to perturbations added to the model initial conditions."

   Reply: The sensitivity test for the size of the verifying region has been shown in this reply. As found in Fig. 1, major patterns of ADSSV with the highest sensitivity would remain the same when the size of the verifying area is increased. Meanwhile, no perturbation needs to be added for the ADSSV calculation in both the forward and backward integrations. The resulted change of the final-time TC location due to the added perturbation in H09 is a totally unrelated issue to the definition and calculation of ADSSV.

3) Second paragraph of the conclusion of H09, "Furthermore, the lack of dynamical interpretation and testing of these sensitivity gradients has allowed these problems to escape notice."

   Reply: It is valuable to conduct the test and validation study, as nicely suggested by H09. Note that W09 has highlighted how ADSSV captures the signals of the influence of the midlatitude trough and the subtropical high prior to the recurvature of Shanshan, and such influence is consistent with the PV analysis. Indeed, the follow-up validation work has been ongoing, and is demonstrated briefly here in section 2d.

4) Third paragraph of the conclusion of H09, "A solution to this problem will take the form of redefining the response functions used to describe the zonal and meridional steering of the TC such that the effect of small perturbations of the final-time location of the TC within the response function box is removed."

   Reply: Again, this is the misunderstanding and misinterpretation from H09 regarding the design and definition of ADSSV in W07 and W09. No perturbation is introduced during the ADSSV calculation in both the forward and backward integrations. As opposed to what is stated in H09, we show that the definition of the response function box is not a problem.

Finally, it should be noted that several targeted observation techniques [i.e., ADSSV; total energy singular vectors (TESVs), from the European Centre for Medium-Range Weather Forecasts (Buizza et al. 2007), Japan Meteorological Agency (Yamaguchi et al. 2009), and NOGAPS models (Peng and Reynolds 2006); the ensemble transform Kalman Filter (ETKF; Bishop et al. 2001; Majumdar et al. 2002); and DLM wind ensemble variance (Aberson 2003)] have been compared in Wu et al. (2009b) to highlight the unique dynamical features affecting TC motion. Wu et al. (2009b) demonstrated that the ADSSV sensitivity shows high similarities to ETKF and also modest similarities to TESVs, indicating these targeted techniques could provide some reliable information to assist in targeted observations.

In the summer of 2008, a major field campaign, The Observing System Research and Predictability Experiment (THORPEX) Pacific Asian Regional Campaign (T-PARC) was conducted, in which four different aircraft (Astra Jet of DOTSTAR, P-3, C-130, and Falcon) were used to investigate the TC genesis, structure change, motion/recurvature (targeted observation), and extratropical transition of TCs (Elsberry and Harr 2008). Some unprecedented data have been collected. It is believed that the data from T-PARC would provide valuable information for assessing targeted observations, and for improving the understanding and forecasts of TCs.

Acknowledgments. The authors especially thank Sharanya J. Majumdar of University of Miami and Carolyn A. Reynolds of Naval Research Laboratory for their helpful comments.

REFERENCES

Aberson, S. D., 2003: Targeted observations to improve operational tropical cyclone track forecast guidance. *Mon. Wea. Rev.,* **131,** 1613–1628.

Bishop, C. H., B. J. Etherton, and S. J. Majumdar, 2001: Adaptive sampling with the ensemble transform Kalman filter. Part I: Theoretical aspects. *Mon. Wea. Rev.,* **129,** 420–436.

Buizza, R., C. Cardinali, G. Kelly, and J.-N. Thepaut, 2007: The value of observations. II: The value of observations located in singular vector-based target areas. *Quart. J. Roy. Meteor. Soc.,* **133,** 1817–1832.

Chan, J. C. L., and W. M. Gray, 1982: Tropical cyclone movement and surrounding flow relationships. *Mon. Wea. Rev.,* **110,** 1354–1374.

Elsberry, R. L., and P. A. Harr, 2008: Tropical cyclone structure (TCS08) field experiment science basis, observational platforms, and strategy. *Asia-Pacific J. Atmos. Sci.,* **44,** 209–231.

Hoover, B. T., 2009: Comments on ''Interaction of Typhoon Shanshan (2006) with the midlatitude trough from both adjoint-derived sensitivity steering vector and potential vorticity perspectives.'' *Mon. Wea. Rev.,* **137,** 4420–4424.

Kleist, D. T., and M. C. Morgan, 2005: Interpretation of the structure and evolution of adjoint-derived forecast sensitivity gradients. *Mon. Wea. Rev.,* **133,** 467–485.

Majumdar, S. J., C. H. Bishop, B. J. Etherton, and Z. Toth, 2002: Adaptive sampling with the ensemble transform Kalman filter. Part II: Field program implementation. *Mon. Wea. Rev.,* **130,** 1356–1369.

Peng, M. S., and C. A. Reynolds, 2006: Sensitivity of tropical cyclone forecasts as revealed by singular vectors. *J. Atmos. Sci.,* **63,** 2508–2528.

Wu, C.-C., T.-S. Huang, W.-P. Huang, and K.-H. Chou, 2003: A new look at the binary interaction: Potential vorticity diagnosis of the unusual southward movement of Typhoon Bopha (2000) and its interaction with Typhoon Saomai (2000). *Mon. Wea. Rev.,* **131,** 1289–1300.

——, and Coauthors, 2005: Dropwindsonde Observations for Typhoon Surveillance near the Taiwan Region (DOTSTAR): An overview. *Bull. Amer. Meteor. Soc.,* **86,** 787–790.

——, J.-H. Chen, P.-H. Lin, and K.-H. Chou, 2007: Targeted observations of tropical cyclone movement based on the adjoint-derived sensitivity steering vector. *J. Atmos. Sci.,* **64,** 2611–2626.

——, S.-G. Chen, J.-H. Chen, K.-H. Chou, and P.-H. Lin, 2009a: Interaction of Typhoon Shanshan (2006) with the midlatitude trough from both adjoint-derived sensitivity steering vector and potential vorticity perspectives. *Mon. Wea. Rev.,* **137,** 852–862.

——, and Coauthors, 2009b: Intercomparison of targeted observation guidance for tropical cyclones in the northwestern Pacific. *Mon. Wea. Rev.,* **137,** 2471–2492.

——, K. K. W. Cheung, and Y.-Y. Lo, 2009c: Numerical study of the rainfall event due to the interaction of Typhoon Babs (1998) and the northeasterly monsoon. *Mon. Wea. Rev.,* **137,** 2049–2064.

Yamaguchi, M., T. Iriguchi, T. Nakazawa, and C.-C. Wu, 2009: An observing system experiment for Typhoon Conson (2004) using a singular vector method and DOTSTAR data. *Mon. Wea. Rev.,* **137,** 2801–2816.